Identification Methodology of Electrical Equivalent Circuit of the Piezoelectric Transformers by FEM

Pigache François, Nadal Clément

Université de Toulouse; INPT, UPS; LAPLACE (Laboratoire Plasma et Conversion d'Energie);
ENSEEIHT, 2 rue Charles Camichel, BP 7122, F-31071 Toulouse cedex 7, France
{pigache}{nadal}@laplace.univ-tlse.fr

Abstract: This paper is about a detailed methodology to identify the Electrical Equivalent Circuit by finite elements method software (Ansys® software) of piezoelectric transformers (PT). The method will be illustrated with a typical Rosen transformer but it is easily applicable to all other architectures of transformers. The identification of parameters is done for the three first longitudinal vibration modes and compared to experimental ones.

Introduction

The piezoelectric transformers are devices operating at particular frequencies due to its resonant properties. Their behaviors are frequently described as a one-dimensional model based on the constitutive equations of linear piezoelectricity and simplified continuum mechanics. The 1D model can be represented by an electrical equivalent circuit for single resonator structure as well as for the piezoelectric transformers (PT). This electrical form is particularly useful for simulation of a complete electrical converter including the device.

By respecting fundamental geometric rules and electrical conditions, (small displacements, predominant dimension, adapted loads…), the volume effect may be neglected and a simple resonant circuit model can give a good accuracy.

The principle of piezoelectric transformer may rely on different piezoelectric couplings depending on the geometry shape and the considered vibration mode. A significant distinction can be made between the low-frequency (extension, flexure, face shear modes) and high-frequency (as thickness shear modes) operating modes. This distinction is especially important in terms of numerical modelling and theoretical assumptions [1], because of the particular cautions required for the latter category.

Each step of the method is detailed in the present paper to obtain the Electrical Equivalent Circuit (EEC) with Ansys® multiphysics software (v11.0). This numerical method can be a convenient alternative way of validation for analytical approach [2] (like Hamilton's principle) also usually used to describe the piezoelectric devices.

Dissipative and thermal effects or nonlinear effects resulting from large displacements or high electric fields are not considered in the present numerical analysis.

At first, the piezoelectric, mechanical and electrical matrices are presented depending on the poling direction. For this reason, the Rosen type transformer is chosen for the demonstration because it presents the particularity of two different poling directions according its receiving and driving elements.

Then, successive steps of static and modal simulations are presented to deduce each equivalent element. The different cautions and assumptions are underlined throughout the demonstration, leading to a controlled and rigorous method. The final results are compared to the experimental results.

1) Presentation of the studied structure

The studied structure is a typical Rosen type transformer as illustrated on Fig. 1. This transformer is commonly used in step-up voltage converter. Its geometry is presented in a Cartesian coordinate system with the origin at the half-width, half-thickness and at the intermediate length between the driving and receiving parts.
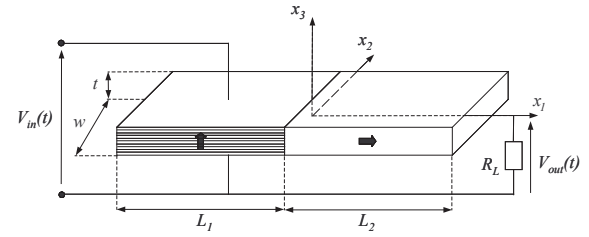

Fig. 1 Typical multilayered Rosen type transformer

As described by Rosen in [3], the driving part is polarized in the thickness direction whereas the receiving part is polarized along the length direction. The driving part can be multilayered in order to increase the step-up voltage ratio. For the requirements of the simulation and final comparison, the dimensions are itemized in TABLE I.

TABLE I.   DIMENSION S OF THE PT

	Definition	*Unit*	*Value*
L_1	Length of driving part	mm	12
L_2	Length of receiving part	mm	13
w	Width	mm	5
t	Thickness	mm	1.7
n	Number of layers in primary part		16

2) Electrical Equivalent Circuit (Mason)

The Electrical Equivalent circuit has been established by Mason in order to describe the electromechanical resonators [4]. This model is easily adapted to the transformers.

Obviously, the 1D Equivalent Circuit is an ideal and simplified interpretation of the double electromechanical conversion in piezo-transformers. In experimental cases, some phenomena can imply significant differences with

the equivalent circuit. As example, a nonuniform or partial polarization of piezoactive elements can produce spurious modes in the vicinity of the main one [5]. The variation of material constants (by thermal effect or ageing) can also lead to inaccuracy. Besides the load connected to the output strongly affects the electromechanical behaviour, leading to a variation of the equivalent parameters.

However, if the mechanical structure can be approximated according to the one- or two-dimensional structural theories (plates, shells, beams and rings) and keeping the device in its linear piezoelectric property, the Mason model brings an accurate approximation of the steady-state electro-mechanical behavior.

Several different equivalent circuits can be found in literature according to the simplifications or circuit reduction. The choice of the electrical scheme mainly depends on the means available for the identification. The equivalent circuit on Fig. 2 is a usual solution for the simulation of piezoelectric transformer in the vicinity of its main resonance frequencies. Each parallel branch corresponds to a particular vibration mode and it requires a specific identification for each one.
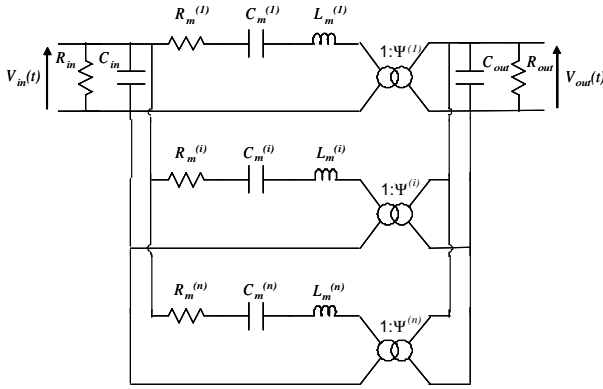

Fig. 2 Electrical Equivalent circuit for clearly distinct vibration modes

On the Fig. 2, L_m and C_m simulate the mechanical resonance, C_{in} and C_{out} are the input and output capacitances respectively. The ideal gain ψ corresponds to the ratio of the two successive electromechanical conversions as follows:

$$\psi = \psi_{in} / \psi_{out} \qquad (1)$$

R_{in} and R_{out} are the dielectric impedances and R_m the mechanical losses. Considering the inaccuracy and the difficulty to express these losses, these parameters will not be simulated with FEM. They are usually expressed by considering an angle of losses for electrical heating and a mechanical quality factor for the damping, experimentally estimated. The influence of losses on the performances of PT is analytically studied in [6].

2) Matrices definition

By default, Ansys® software presents a particular matrices order slightly different from the IEEE standard one (see Ansys® help). Additionally, the poling axis is initially defined in the z direction as the conventional definition.

As a consequence, the matrices are reminded below in the case of a PZT* ceramic polarized in the different directions according to the Ansys® definition. The numerical values of parameters are collected in TABLE II.

Poling in Z-direction

$$[c]_Z^E = \begin{bmatrix} c_{11}^E & c_{12}^E & c_{13}^E & 0 & 0 & 0 \\ & c_{11}^E & c_{13}^E & 0 & 0 & 0 \\ & & c_{33}^E & 0 & 0 & 0 \\ & & & c_{66}^E & 0 & 0 \\ & sym & & & c_{44}^E & 0 \\ & & & & & c_{44}^E \end{bmatrix}$$

$$[e]_Z^t = \begin{bmatrix} 0 & 0 & 0 & 0 & 0 & e_{15} \\ 0 & 0 & 0 & 0 & e_{15} & 0 \\ e_{31} & e_{31} & e_{33} & 0 & 0 & 0 \end{bmatrix}$$

$$[\varepsilon]_Z = \begin{bmatrix} \varepsilon_{11}^S & 0 & 0 \\ & \varepsilon_{11}^S & 0 \\ & & \varepsilon_{33}^S \end{bmatrix}$$

Poling in Y-direction

$$[c]_Y^E = \begin{bmatrix} c_{11}^E & c_{13}^E & c_{12}^E & 0 & 0 & 0 \\ & c_{33}^E & c_{13}^E & 0 & 0 & 0 \\ & & c_{11}^E & 0 & 0 & 0 \\ & & & c_{44}^E & 0 & 0 \\ & sym & & & c_{44}^E & 0 \\ & & & & & c_{66}^E \end{bmatrix}$$

$$[e]_Y^t = \begin{bmatrix} 0 & 0 & 0 & e_{15} & 0 & 0 \\ e_{31} & e_{33} & e_{31} & 0 & 0 & 0 \\ 0 & 0 & 0 & 0 & e_{15} & 0 \end{bmatrix}$$

$$[\varepsilon]_Y = \begin{bmatrix} \varepsilon_{11}^S & 0 & 0 \\ & \varepsilon_{33}^S & 0 \\ & & \varepsilon_{11}^S \end{bmatrix}$$

Poling in X-direction

$$[c]_X^E = \begin{bmatrix} c_{33}^E & c_{13}^E & c_{13}^E & 0 & 0 & 0 \\ & c_{11}^E & c_{12}^E & 0 & 0 & 0 \\ & & c_{11}^E & 0 & 0 & 0 \\ & & & c_{44}^E & 0 & 0 \\ & sym & & & c_{66}^E & 0 \\ & & & & & c_{44}^E \end{bmatrix}$$

$$[e]_X^t = \begin{bmatrix} e_{33} & e_{31} & e_{31} & 0 & 0 & 0 \\ 0 & 0 & 0 & e_{15} & 0 & 0 \\ 0 & 0 & 0 & 0 & 0 & e_{15} \end{bmatrix}$$

$$[\varepsilon]_X = \begin{bmatrix} \varepsilon_{33}^S & 0 & 0 \\ & \varepsilon_{11}^S & 0 \\ & & \varepsilon_{11}^S \end{bmatrix}$$

* The PZT ceramic is assimilated to the "6mm" crystal class in the hexagonal system leading to symmetry and simplification of matrices.

Fig. 4 Selection of different groups of nodes

Static analysis

The static analysis gives the capacitances of the driving and receiving parts resulting from the dielectric property of the ceramic.

The method consists in the application of voltage condition on electrodes (typically 1V) then the reading of calculated quantity of charges. It gives the static capacitor value by the simple following expression:

$$C_{static} = q_c / V \qquad (2)$$

with q_c the quantity of charges and V, the applied voltage. This result is retrieved by the following APDL line code:

	APDL code
*get, qc, node, group_name,rf, amps Cstatic = abs(qc) ! C = Q/V, where V = 1 Volt	

However, this calculated capacitor does not correspond to the clamped capacitor illustrated on Fig. 2 by C_{in} and C_{out}. Indeed, the piezoelectric effect implies a different equation balanced by the coupling factor as follows:

$$C_{clamped} = n^2 . C_{static} . (1 - k_{ij}^2) \qquad (3)$$

with k_{ij} the coupling factor of the considered mode (ie: k_{31} transversal coupling factor in driving part). In addition, if the driving part is laminated with n layers, the equivalent capacitor is proportional to the square of numbers of layers as expressed above. This static analysis is successively used to define both capacitances. The obtained values are collected in TABLE IV like all the other numerical results.

Modal analysis

The modal analysis gives the natural resonant frequencies and mode shapes of the structure. It must be reminded that this analysis presents an indetermination for a complete identification. Consequently, the analysis is necessarily relative to a chosen convention. For this reason, two different normalizations are proposed in the solution menu of Ansys® (to unity or to the mass matrix).

As the electrical loads influence the electromechanical behavior, the choice of electrical conditions (open or short-circuited) will lead to different values of identified parameters. These conditions must be chosen according to the expected operating conditions. In the present case, it has been chosen that the output will be connected to high impedance. As a consequence, the identification of parameters will be undertaken under open receiving electrode.

1) Short-circuited analysis

The first objective of the modal analysis is to identify the

TABLE II. CERAMIC MATERIAL PROPERTIES [7]

	Definition	Unit	Value
c_{11}^E	Stiffness at constant electric field E	N. m^{-2}	1.68E+11
c_{12}^E			1.10E+11
c_{13}^E			9.99E+10
c_{44}^E			3.01E+10
c_{66}^E			2.88E+10
e_{31}	Piezoelectric constants	C.m^{-2}	-2.8012
e_{15}			9.8568
e_{33}			14.6913
ε_{11}^S	Relative permittivity at constant strain S		829
ε_{33}^S			701
ρ	Density	kg.m^{-3}	7700
k_{31}	Transversal coupling factor		0.330
k_{33}	Longitudinal coupling factor		0.678

3) Geometry Building set

The transformer is drawn with classical design operators (block volume BLC4 here). The receiving and driving parts are drawn as single blocks (Fig. 3) even if multilayers are used. The laminated part is considered as a perfect mechanical association and the influence of layers will be considered later in calculations.

The meshing must satisfy a sufficient precision as usually in this kind of electromechanical simulations. The size of elements must be chosen in accordance with the volume of interest.
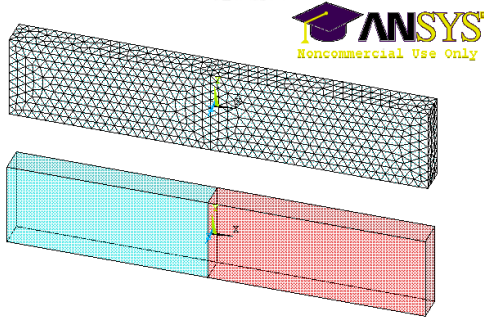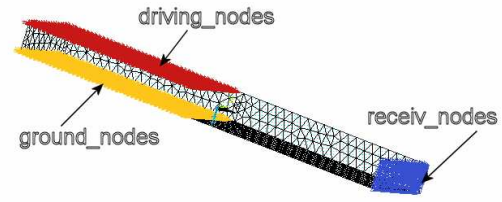
Fig. 3 Design of Rosen PT and meshing

In the present case, no mechanical limit conditions are fixed: the device is under free-free mechanical boundary conditions.

About the external electrical conditions, several groups of nodes must be defined in order to materialize the different electrodes and apply to them the voltage conditions. Three distinct electrodes are defined. Two electrodes are materialized on the largest areas of the driving part and one at the end of the receiving part as illustrated on following Fig. 4. After selected the required nodes, each group is defined by the following APDL codes:

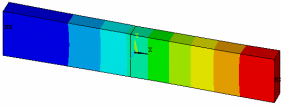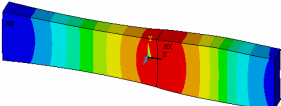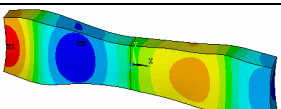|	APDL code
cp,1,volt,all *get,group_name,node,0,num,min	

eigenfrequencies of the mechanical structure. Thus, the different electrodes are fixed to 0 volt in order to avoid the electric field appearing between them and consequently suppress the dielectric aspect of the material. This condition of simulation gives the series resonant frequencies f_s.

The constraint of 0 volt is applied to the groups of nodes previously defined as follows:

APDL code
d,*driving_nodes*,volt,0
d,*receiv_nodes*,volt,0
d,*ground_nodes*,volt,0 ! apply constraint 0V at nodes

As results, the set of vibration modes are obtained with the eigenfrequencies. All mode shapes are indistinctly listed. A selection of specific modes must be led to keep only the interesting modes able to be reduced to 1D model. In present case, the interesting modes for an efficient step-up voltage are only the three first ranks of vibration modes along the main dimension *i.e.* in the *x* direction. The visual 3D results of selected longitudinal modes are listed in TABLE III, distinguished by their ratio of the wavelength λ in *x* direction.

TABLE III.   3D RESULTS OF THREE FIRST LONGITUDINAL MODES

Read-out U_x component of displacement	Mode rank
	$\lambda/2$ mode
	λ mode
	$3\lambda/2$ mode

In addition, the displacement along *x*-axis can be more visible by employing the "path operation" operator which gives the normalized waveforms shown on Fig. 5.
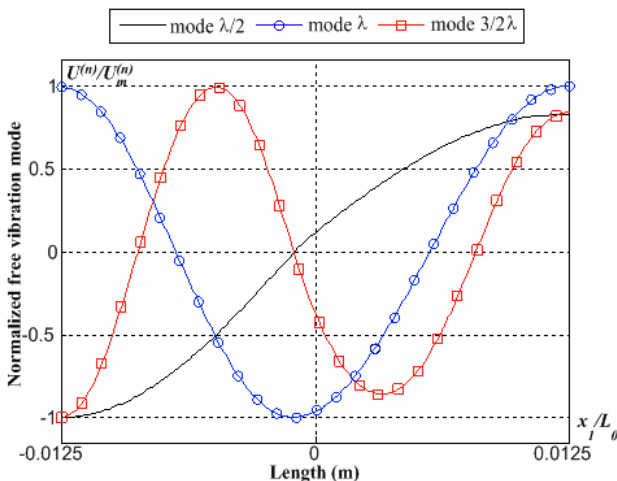

Fig. 5 Displacement along the length for the three first longitudinal modes

The non-homogeneous stiffnesses of both parts along the

x-axis influence the position of the zero crossing. It is especially visible with the $\lambda/2$ mode on Fig. 5 where the zero crossing does not appear at the middle of the length. This is an additional advantage of the analysis by numerical method because this non homogeneous property is often neglected by the analytical approach, leading to an additional precision error.

NB: At this step of the study, no comparison of wave amplitudes can be done in this condition of simulation (free vibration). The comparison between modes and complementary results will be available by a forced vibration analysis (harmonic analysis). However, the harmonic analysis must be led with particular caution. Indeed, due to the non-consideration of damping effect, the harmonic result tends to an infinite value at the exact resonance frequency and subsequently unrealistic. This simulation will be strongly dependent on the frequency step and consequently, unexploitable without the consideration of the damping coefficient.

3) Partial short-circuited analysis

The modal analysis with a different electrical condition (open or short-circuited parts) gives additional information in order to complete the identification of electrical elements. Typically, the modal analysis in electrical condition of short-circuited primary side and opened secondary one leads to the value of parallel resonance frequencies f_p.

4) Calculations of modal stiffness, modal mass and modal electromechanical conversion factor

The calculation of the different elements is relative to the selected generalized coordinates. As commonly in literature, the generalized coordinates which described the mechanical energy of the system is the maximal amplitude (or RMS amplitude) displacement noted q_U. As a consequence, all parameters are relatively deduced to this quantity, whatever the normalization criterion is.

Ansys® determines the kinetic and strain energies with the elements table calculation. By definition, it is possible to describe these mechanical energies according to q_U, the generalized coordinate, as follows:

	Ansys® command	Analytic expression
Kinetic Energy	KENE	$T = \dfrac{1}{2}M\dot{q}_U{}^2 = \dfrac{1}{2}Mq_U{}^2\omega^2$
Strain energy	SENE	$U = \dfrac{1}{2}Kq_U{}^2$

where *M* and *K* are respectively the modal mass and the modal stiffness. These terms are successively deduced for each considered vibrations mode.

It is decided to calculate the modal parameters with the open electrode at the receiving part. This decision is motivated by the reason that the operating point of the transformer is at high load impedance. As a consequence, two different methods are necessary to deduce both electromechanical conversion factors.

The electromechanical conversion factor corresponds to the ratio between the electrical quantity of charge q_c and the quantity of displacement q_U.

Because the primary side is short-circuited, the quantity of charge is available and the input conversion factor ψ_{in} can be deduced according to the following APDL code:

APDL code

```
*get, qc, node, driving_nodes, rf, amps !quantity of charge
nsort,U,X
*get,maxUx,sort, ,max  ! max displacement
*get,minUx,sort, ,min  ! min displacement

*if, abs(minUx), gt, abs(maxUx), then, DUx=minUx
*else DUx=maxUx
*endif
psi_in=n*qc/DUx
```

The input conversion factor is directly proportional to the number of laminated layers. Concerning the second electromechanical factor ψ_{out}, it is not possible to measure the quantity of charge because it is in open circuit. Physically, the piezoelectric effect implies a polarization leading to the appearance of output voltage at the secondary electrode. According to the expanded Electrical Equivalent Circuit, this output voltage is dependent on the amplitude quantity by the following equation:

$$\psi_{out} = C_{out}.V_{out}/q_U \qquad (4)$$

Since the output capacitance and the amplitude quantity have been previously determined, the reading of the output voltage V_{out} finally leads to the output electromechanical conversion factor. APDL code is expressed below:

APDL code

```
nsort, volt
*get, vout ,node, receiv_nodes, volt
psi_out=Cout*vout/DUX
```

The modal parameters are all determined (except the unconsidered damping parameters and losses). Finally, the equivalent parameters can be calculated according to the following relations issued from the reduction electrical circuit:

$$C_m = \psi_{in}^2/K \qquad L_m = \psi_{in}^2.M \qquad \psi = \frac{\psi_{in}}{\psi_{out}} \qquad (5)$$

Results and discussion

The complete analytical, numerical and experimental studies have been done about this Rosen piezoelectric transformer in [2]. The campaign of numerical simulations finally gives all the parameters collected in TABLE IV. The experimental results are also presented in parentheses beside the numerical values. The experimental identification relies on the classical method detailed in [8]. This experimental identification is done with the low voltage impedance analyzer HP4294. Globally, the results of simulation show an excellent accuracy compared to the experimental measurements. The notice (-) concerns the unreachable parameters by experimental measurements.

It may be noticed that the sign of the ideal voltage ratio ψ depends on the conventional sign of the chosen waveform. However, the successive alternation of sign at each mode is an observable physical property.

The ideal voltage gain ψ of the $\lambda/2$ longitudinal mode presents the largest difference with the experimental measurement whereas the other gains are quite accurate.

Fig.6 and Fig.7 give electrical characteristics of the PT on a wide frequency range including the three longitudinal vibration modes. Numerical and experimental curves are both obtained from the simulation of the Electrical Equivalent Circuit previously identified with an output load at 500kΩ.

Mechanical damping and electrical losses are included in the model of simulation by a conventional mechanical quality factor Q_m and angle of losses $tan(\varphi)$.

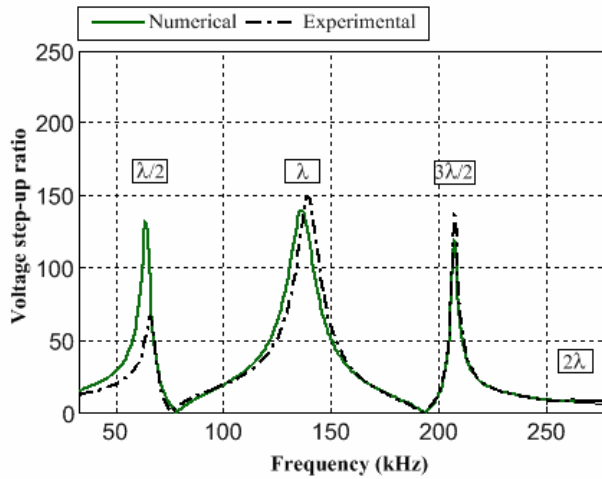|	Mode $\lambda/2$		Mode λ		Mode $3\lambda/2$	
	Simulation	(Exp.)	Simulation	(Exp.)	Simulation	(Exp.)
f_s [kHz]	61.88	(63.37)	124.87	(127.92)	203.57	(203.98)
f_p [kHz]	70.47	(69.60)	141.25	(140.40)	206.50	(207.15)
M [g]	0.67	(-)	0.762	(-)	0.589	(-)
K [GN/m]	0.131	(-)	0.60	(-)	0.991	(-)
L_m [mH]	0.852	(1.06)	0.33	(0.347)	2.935	(2.056)
C_m [nF]	5.984	(5.94)	3.814	(4.45)	0.202	(0.296)
ψ_{in} [C/m]	0.887	(-)	1.513	(-)	0.448	(-)
ψ_{out} [C/m]	-9.477e-3	(-)	2.403e-2	(-)	-1.21e-2	(-)
ψ	-93.58	(47.98)	62.95	(63.82)	-37	(44.05)
C_{in} [nF]	96.8	(97.13)	96.8	(98.05)	96.8	(107.2)
C_{out} [pF]	4.34	(5.03)	4.34	(5.47)	4.34	(4.79)

Fig. 6 Voltage ratio obtained by experimental and numerical identification of EEC
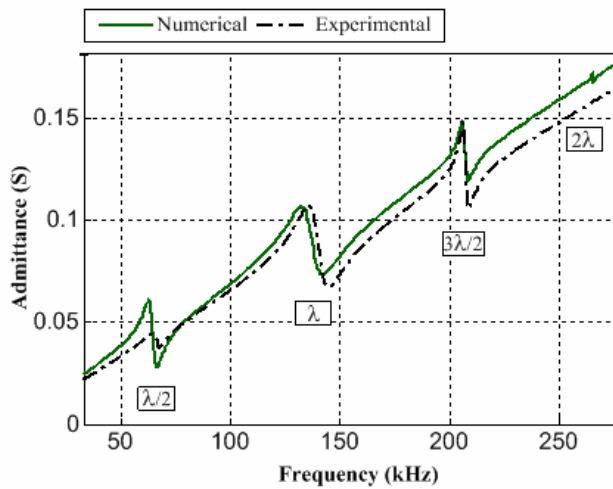

Fig. 7 Input admittance obtained by experimental and numerical identification of EEC

Conclusion

This paper deals with a methodology for the identification of the Electrical Equivalent Circuit by finite elements method applied to the piezoelectric transformer. This identification is carried out with the Ansys® multiphysics software. The structure of matrices is presented according to the different poling direction of material by respecting the specific ansys matrices order. Then, the static and modal analyses are presented and some APDL lines of code are given to help during the post-processing calculations. Even if a harmonic analysis is available with ansys® software, it does not bring additional elements for equivalent circuit identification due to the not considered damping and losses.

Successive simulations are presented in order to obtain the main parameters of the equivalent circuit. This method helps to validate the 1D model approximation and to define its limit of validity and so whatever the structure of the transformer is. This approach is pertinent at the condition to satisfy the one- or two- dimensional structural theories.

References

[1] J. Yang, "Piezoelectric transformer structural modeling – A review", IEEE Trans. on Ultrasonics, Ferroelectrics and Frequency Control, vol. 54, Issue 6, pp.1154-1170, June 2007.

[2] C. Nadal , F. Pigache, "Multimodal electromechanical model of piezoelectric transformers by Hamilton's principle", Trans. on Ultrasonics, Ferroelectrics and Frequency Control, vol. 56 , Issue 11, pp. 2530-2543, DOI 10.1109/TUFFC.2009.1340, November 2009.

[3] C. Rosen, "Ceramic transformers and filters", in Proc. Electronic components Symp., pp. 205-211, 1956.

[4] W. P. Mason, Electromechanical Transducers and Wave Filters, Princeton, NJ, Van Nostrand, 1948.

[5] T. Tsuchiya, Y. Kagawa, N. Wakatsuki, and H. Okamura, "Finite element simulation of piezoelectric transformers", IEEE Trans. on Ultrasonics, Ferroelectrics and Frequency Control, vol. 48, Issue 4, pp. 872-878, July 2001.

[6] V.L. Karlash, "Influence of Energy Losses on the Performance of a Piezoelectric Transformer Plate", International Applied Mechanics, Vol. 39, n° 8, DOI 10.1023/A:1027477118684, août 2003

[7] J. Fernandez Lopez, "Modeling and optimisation of linear piezoelectric motors", PhD. thesis, Ecole Polytechnique Fédérale de Lausanne, Switzerland, November 2006.

[8] R.L. Lin, "Piezoelectric transformer characterization and application of electronic ballast", Ph.D. Dissertation, Virginia Tech, November 2001.